ADVANCED MATERIALS

using a commercially available capacitance meter operating at 800 Hz (Iso-Tech 9023). The capacitors were connected to the capacitance meter via Karl Süss MicroTec PH100 miniature probe heads. The measurement was repeated on a minimum of six spots located on the whole length of anodized part of the foil. The leakage measurements were performed directly after capacitance measurements using the same connections. The bottom (Ti) electrode was biased either positively (as it was during anodization) or negatively (as it would be in a p-type transistor). Subsequently, organic field-effect transistors were fabricated by evaporating pentacene (97 %, Aldrich, used as received) under a high vacuum $< 5 \times 10^{-7}$ torr with a rate of 0.3 nm s^{-1} at room temperature. The pentacene film thickness measured with a Dektak profilometer was ~50 nm. The transistors were completed by evaporation of gold source and drain contacts through a shadow mask on the top of the pentacene layer. The channel width and length was 2 mm and 25 μm, respectively. Characterization was performed at ambient conditions without any special precautions. Two Keithley 2400 source/measure units were used to control source–drain (V_{SD}) and gate (V_G) voltages.

Received: May 21, 2004
Final version: July 12, 2004

[1] A. I. Kingon, J. P. Maria, S. K. Streiffer, *Nature* **2000**, *406*, 1032.
[2] T. Inoue, T. Ohsuna, Y. Obara, Y. Yamamoto, M. Satoh, Y. Sakurai, *Jpn. J. Appl. Phys., Part 1* **1993**, *32*, 1765.
[3] L. Manchanda, M. Gurvitch, *IEEE Electron Device Lett.* **1988**, *9*, 180.
[4] K. P. Pande, V. K. R. Nair, D. Gutierrez, *J. Appl. Phys.* **1983**, *54*, 5436.
[5] P. K. Roy, I. C. Kizilyalli, *Appl. Phys. Lett.* **1998**, *72*, 2835.
[6] H. Kim, D. C. Gilmer, S. A. Campbell, D. L. Polla, *Appl. Phys. Lett.* **1996**, *69*, 3860.
[7] E. Becker, R. Parashkov, G. Ginev, D. Schneider, S. Hartmann, F. Brunetti, T. Dobbertin, D. Metzdorf, T. Riedl, H.-H. Johannes, W. Kowalsky, *Appl. Phys. Lett.* **2003**, *83*, 4044.
[8] J. Tate, J. A. Rogers, C. D. W. Jones, B. Vyas, D. W. Murphy, W. Li, Z. Bao, R. E. Slusher, A. Dodabalapur, H. E. Katz, *Langmuir* **2000**, *16*, 6054.
[9] Y. Iino, Y. Inoue, Y. Fujikake, H. Sato, M. Kawakita, S. Tokito, H. Kikuchi, *Jpn. J. Appl. Phys., Part 1* **2003**, *42*, 299.
[10] L. A. Majewski, R. Schroeder, M. Grell, *J. Phys. D: Appl. Phys.* **2004**, *37*, 21.
[11] H. Y. Choi, S. H. Kim, J. Jang, *Adv. Mater.* **2004**, *16*, 732.
[12] A. W. Hassel, D. Diesing, *Thin Solid Films* **2002**, *414*, 296.
[13] *Technical Notes of Aluminum Electrolytic Capacitors,* Technical Note 8101C, Nichicon America, Schaumburg, IL.
[14] S. A. Campbell, H. S. Kim, D. C. Gilmer, B. He, T. Ma, W. L. Gladfelter, *IBM J. Res. Dev.* **1999**, *43*, 383.
[15] R. B. van Dover, *Appl. Phys. Lett.* **1999**, *74*, 3041.
[16] J. Veres, S. D. Ogier, S. W. Leeming, D. C. Cupertino, *Adv. Funct. Mater.* **2003**, *13*, 199.
[17] J. Veres, S. Ogier, S. Leeming, D. Cupertino, S. M. Khaffaf, G. Lloyd, *Proc. SPIE-Int. Soc. Opt. Eng.* **2003**, *5217*, 147.
[18] T. W. Kelly, D. V. Muyres, P. F. Baude, T. P. Smith, T. D. Jones, *Mater. Res. Soc. Symp. Proc.* **2003**, *771*, L6.5.
[19] Y. Fujisaki, Y. Inoue, T. Kurita, S. Tokito, H. Fujikake, H. Kikuchi, *Jpn. J. Appl. Phys., Part 1* **2004**, *43*, 372.
[20] J. Lee, K. Kim, J. H. Kim, S. Im, D. Y. Jung, *Appl. Phys. Lett.* **2003**, *82*, 4169.
[21] R. Schroeder, L. A. Majewski, M. Grell, *Appl. Phys. Lett.* **2003**, *83*, 3201.
[22] S. M. Sze, *Physics of Semiconductor Devices*, 2nd ed., Wiley-VCH, New York **1981**, p. 447.
[23] J. P. Coling, J. W. Park, W. Xiong, *IEEE Electron Device Lett.* **2003**, *24*, 515.
[24] G. Wang, D. Moses, A. J. Heeger, H. M. Zhang, M. Narasimhan, R. E. Demaray, *J. Appl. Phys.* **2004**, *95*, 316.

High Efficiency and Quadratic Nonlinear Optical Properties of a Fully Optimized 2D Octupolar Crystal Characterized by Nonlinear Microscopy**

By *Véronique Le Floc'h*, *Sophie Brasselet*,* *Joseph Zyss*, *Bong Rae Cho*,* *Sang Hae Lee*, *Seung-Joon Jeon*, *Minhaeng Cho*, *Kil Sik Min*, and *Myunghyun Paik Suh*

The study of octupolar molecules[1,2] has opened up new research directions in the design and synthesis of new families of molecules that have large nonlinear optical susceptibilities (hyperpolarizabilities), β, with possible applications in optical and opto-electronic devices. Among the advantages of octupolar structures is that they have a broader range of nonlinear tensorial coefficients β_{ijk} (where i, j, k are the molecular-frame indices) compared to earlier 1D schemes,[3] which provides an optimum nonlinear efficiency with a polarization-independent second-harmonic response to incident light. Optimization at the molecular level has made great progress, as exemplified by the established structure–property relationship of two-dimensional octupoles and by the development of highly efficient molecules.[4–7] Different strategies have been proposed to obtain a significant bulk second-order optical nonlinearity, $\chi^{(2)}$, by the non-centrosymmetric alignment of octupoles such as optical poling in polymers,[8] supramolecular arrangement,[9–11] and crystal engineering.[12] Although the crystalline structures would be more advantageous in terms of stability, achieving three-dimensional octupolar geometry at the mac-

[*] Dr. S. Brasselet, Dr. V. Le Floc'h, Prof. J. Zyss
Laboratoire de Photonique Quantique et Moléculaire (UMR 8537)
Institut d'Alembert (IFR 121)
Ecole Normale Supérieure de Cachan
61 avenue du Président Wilson
F-94235 Cachan Cedex (France)
E-mail: sophie.brasselet@lpqm.ens-cachan.fr
Prof. B. R. Cho, Dr. S. H. Lee, Prof. S.-J. Jeon
Molecular Opto-Electronics Laboratory
Department of Chemistry and Center for Electro- and Photo-Responsive Molecules, Korea University
1-Anamdong, Seoul 136-701 (Korea)
E-mail: chobr@korea.ac.kr
Prof. M. Cho
Department of Chemistry and Center for Multidimensional Spectroscopy, Korea University
1-Anamdong, Seoul 136-701 (Korea)
Dr. K. S. Min, Prof. M. P. Suh
Department of Chemistry, Seoul National University
Seoul 151-744 (Korea)

[**] This work is supported by a NRL grant, Creative Research Initiative Program (KISTEP), and KOSEF. SHL was supported by the BK21 scholarship. We thank Prof. H. Ito (Tohoku University, Japan) for having provided the DAST crystal, and Prof. J.-F. Roch for helpful discussions. Supporting Information is available online from Wiley InterScience of from the author.

  DOI: 10.1002/adma.200400451

roscopic scale is non-trivial, and up to now, to the best of our knowledge, octupolar crystals with large bulk nonlinearities have not been reported. Recently, we demonstrated that 1,3,5-tricyano-2,4,6-tris(*p*-diethylaminostyryl)benzene (TTB) and its derivatives exhibit large first hyperpolarizabilities and significant second-harmonic generation (SHG) in the powder state.[13] However, the origin of the bulk nonlinearity at the macroscopic level conjectured in the literature[1] has not been experimentally investigated. In this work, we show that the TTB crystal has a non-centrosymmetric octupolar structure, which facilitates optimal transfer of the molecular hyperpolarizability components to the macroscopic level. Indeed, in other types of structures such as dipolar or multipolar crystals, the macroscopic symmetry is often different from the molecular one, which results in a decrease in efficiency upon projecting the molecular tensorial components onto the macroscopic frame. The TTB crystal, which does not suffer from such drawbacks, consequently exhibits a very large bulk nonlinearity.

The TTB single crystals were obtained by slowly evaporating a saturated solution of TTB in CH_2Cl_2–EtOEt. The crystals were cylindrical in shape with hexagonal cross-sections, and their sizes ranged from several micrometers to several millimeters. The X-ray structure of the octupolar molecule is shown in Figure 1a; four benzene moieties lie in the same plane, with dihedral angles of ca. 30° between the central and

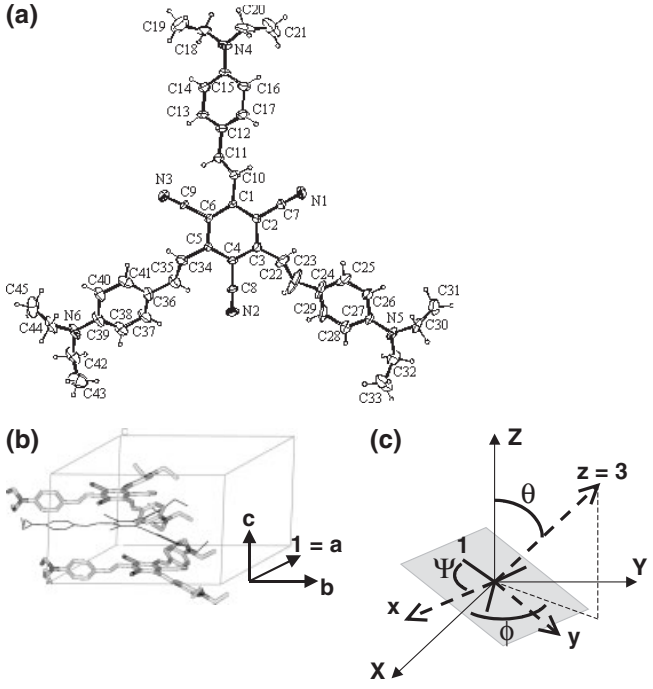

Figure 1. a) TTB structure drawn using the software ORTEP. b) Unit-cell structure of the TTB crystal. The 1-axis is chose to be parallel to one of the C_2-axes. c) Definition of the Euler angles (θ,ϕ,ψ) in the macroscopic framework (*X*,*Y*,*Z*), given the orientation of the unit-cell framework (1,2,3): the (θ, ϕ) angles define the orientation of the *x*-*y* molecular plane in the macroscopic (*X*,*Y*,*Z*) frame. The TTB molecules, represented by the plain lines, lie in the *x*-*y* plane, with an orientation angle ψ between the *x*- and 1-axes.

peripheral phenyl rings. Tertiary amine nitrogen atoms exhibit sp^2 hybridization instead of sp^3 so that the whole molecule, except for the terminal methyl groups, lies approximately in one plane. The important consequences of this planarity are i) an increased molecular hyperpolarizability value, β, due to efficient charge transfer from the donor to the acceptor groups and ii) a potentially non-centrosymmetric arrangement of the molecules in the crystal lattice, induced by the enhanced π–π interlayer stacking interactions.

The three-dimensional arrangement of TTB in the crystal unit cell is shown in Figure 1b. It consists of three molecules packed along the *c*-axis with a slight offset. The π–π stacking interactions between adjacent molecules stacked in neighboring layers play a crucial role in the formation of the non-centrosymmetric crystal.[14] Intermolecular herringbone π–π interactions between the phenyl groups in the side chains of neighboring molecules within the same layer can also contribute to the final three-dimensional non-centrosymmetric arrangement. This confirms that a planar octupolar molecule with long "arms" containing aromatic rings that can induce non-negligible π–π interactions (and thus minimize any void volume in a given unit cell) is most likely to form a non-centrosymmetric crystal, based on the Kitaigorodskii closest-packing paradigm for molecular crystal structures.[15]

To confirm optically the octupolar crystalline structure and determine the molecular arrangement inside the submillimeter-sized crystal, we applied a polarized nonlinear microscopy analysis technique combining second harmonic generation (SHG) and two-photon fluorescence (TPF). This unique methodology is based on the interplay of two complementary optical effects that have recently been shown to allow the resolution of complex molecular arrangements.[16] The TTB crystal, lying on a microscope slide, was illuminated in the nonlinear microscopy setup either sideways along its cylindrical axis or from the top along its hexagonal face. The IR exciting beam originating from a femtosecond titanium/sapphire (Ti:Sa) laser (150 fs, 86 MHz repetition rate) was focused onto the crystal using a high-numerical-aperture (high-NA) objective (NA: 1.4; ×60) with a spatial resolution of about 400 nm and a typical pulse energy of the order of 3 pJ, at a fundamental wavelength of 1028 nm. The emitted TPF and SHG signals were collected by the same objective. A beam splitter directed the emitted signals to a spectrograph and the resulting spectrum exhibited the SHG peak at half the incident wavelength (514 nm), well-separated from the fluorescence emission band, which was around 710 nm (see Supporting Information). The SHG or TPF signals were therefore easily detectable using appropriate spectral filters. The signals were then directed to a polarization analysis set-up operating in the photon-counting regime, the perpendicularly polarized signals being simultaneously recorded on two avalanche photodiodes. Two perpendicular polarization states were thus detected, while the incident polarization was rotated in the plane of the microscope slide (*X*-*Y* plane) using a rotating half-wave plate (Fig. 1c). The incident polarization direction, $\boldsymbol{E}$, is defined by the angle $\Phi = (\boldsymbol{X},\boldsymbol{E})$, (i.e., the angle between

ADVANCED MATERIALS

X and ***E***) which was varied from 0° to 360°. Polarization calibrations suggested that ellipticity and dichroism parameters had to be duly taken into account, because of the reflection of the incident beam on the dichroic mirror.[16]

The TPF and SHG polarization responses can be expressed as a function of the unit-cell orientation (θ,ϕ,ψ) within the crystal as described in Figure 1c. The corresponding intensities, S, analyzed along a given direction, I, are given by[16]

$$S_I^{\mathrm{TPF}} = \alpha_{II} \sum_{JKLM} \gamma_{JKLM} \overline{E_J E_K E_L E_M}(\Phi) \quad (1)$$

and

$$S_I^{\mathrm{SHG}} = \sum_{JK} \beta_{IJK} \beta_{ILM} \overline{E_J E_K E_L E_M}(\Phi) \quad (2)$$

where the indices I, J, K, L, and M refer to coordinates in the macroscopic framework and E_x ($x = J, K, L, M$) is the x-component of the incident field. The notation $\overline{(\cdots)}$ denotes the temporal average over the detector integration time of $(\cdots)$, while α represents the one-photon emission tensor, γ the two-photon excitation tensor, and β the hyperpolarizability tensor. These tensors can be expressed in the macroscopic framework using the purely additive oriented gas model.[17] In such a scheme, $\alpha_{IJ}(\theta,\phi,\psi) = \sum_{ij} \alpha_{ij} \cos(i,I) \cos(j,J)$ (and similar expressions for the γ and β tensors), with $\cos(i,I)$ being the projections of the $i = (1,2,3)$ axes on the $I = (X,Y,Z)$ axes, which are dependent on (θ,ϕ,ψ). The application of such a model, which a priori ignores intermolecular interactions, is justified by the experimental results. Assuming an octupolar planar symmetry of the molecular arrangement within the TTB crystal, the unit-cell tensor coefficients α_{ij}, β_{ijk}, and γ_{ijkl}, are only limited to $\alpha_{11} = \alpha_{22} = 1/\sqrt{2}\|\alpha\|$ (with $\|\alpha\| = \sum_{ij} \alpha_{ij}^2$), $\gamma_{1111} = \gamma_{2222} = 0.612\|\gamma\|$, $\gamma_{1122} = \gamma_{2211} = \gamma_{1221} = \gamma_{2112} = \gamma_{2121} = \gamma_{1212} = \gamma_{1111}/3 = 0.204\|\gamma\|$, and $\beta_{111} = -\beta_{122} = -\beta_{212} = -\beta_{221} = 0.5\|\beta\|$. By fitting the (θ,ϕ,ψ) values to the experimental data with the variable Φ, it is possible to confirm the octupolar structure of the crystalline unit cell as well as to determine the orientation of the octupoles within the crystal lattice.

The TPF and SHG signals were first analyzed in a configuration where the crystal lay along one of its sides with different orientations in the X–Y plane, as displayed in Figure 2. In this configuration, the best agreement with the data was obtained when $\theta = 90°$, which corresponds to the case where the octupole planes lie edgeways, i.e., perpendicular to the X–Y plane. The orientation of the crystal side in the sample plane was then fully defined solely by the angle ϕ , while the in-plane ψ angle became irrelevant. The crystal orientation angles retrieved from the fits corresponded to the expected orientations in the (X,Y,Z) framework. The polarization features were characteristic of a planar-molecular stacking direction in the crystal. Indeed, the two-lobed pattern was perpendicular to the cylindrical axis and followed the rotation of the crystal, which is a signature of the anisotropism of the projection of octupoles lying perpendicular to the sample plane and parallel to the hexagonal face.

In contrast to the previously depicted "sideways" configurations, the TPF and SHG polarization responses of the crystal lying on its hexagonal face exhibited four-lobed patterns (Fig. 3). These patterns remained invariant for any π/3 rotation of the crystal in its plane. Such a result provides clear evidence of the threefold symmetry in the plane of the hexagonal face, which stands out as a clear characteristic feature of octu-

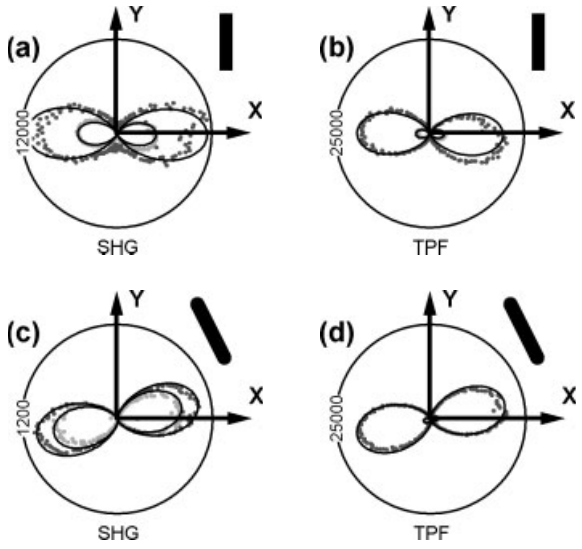

Figure 2. Polar diagrams representing the SHG (a,c) and the TPF (b,d) intensities as functions of the incident polarization angle Φ. Experimental data S_X (in dark gray) and S_Y (in light gray) in counts/100 ms were obtained using an incident-beam power of 200 μW. The continuous lines correspond to the intensity fits with the following orientation parameters: a,c) (90°,30°,–5°) and b,d) (90°,30°,88°). An ellipticity parameter of $\varepsilon = 1.57$ rad and an amplitude dichroism factor $\delta = -0.02$ at 1028 nm [16] accounted for the incident-field ellipticity. The crystal directions are represented by the dark rectangles.

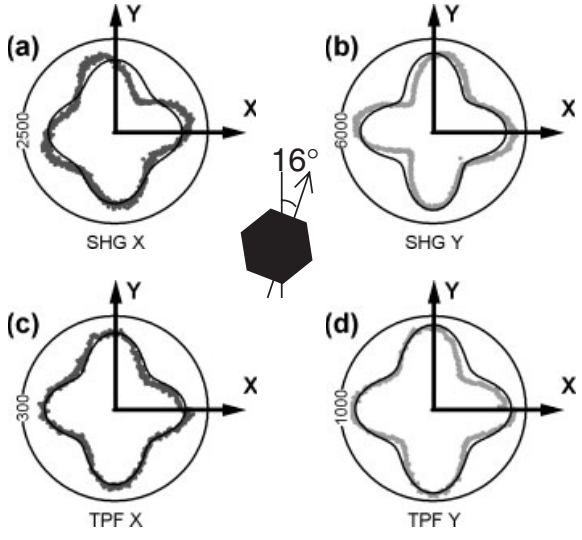

Figure 3. Polar diagrams representing the SHG (a,b) and the TPF (c,d) intensities as functions of the Φ angle with the crystal lying on its hexagonal face. Experimental data S_X (in dark gray) and S_Y (in light gray) in counts/100 ms were obtained using an incident beam power of 56 μW. The continuous lines correspond to the intensity fits with the Euler angles (0°,0°,16°).

polar molecular structures. Note that the sum of the optical signals for the two X and Y analysis directions gives, for both SHG and TPF, four-lobed patterns oriented along the X- and Y-directions, instead of the circular pattern expected from the polarization-independent SHG response for octupolar symmetry.[18] This deviation is due to the ellipticity of the incident laser beam introduced by the dichroic mirror, which affected intermediate polarizations. The fits of the experimental data were obtained with $\theta = 0°$, as expected, $\phi = 0°$, and $\psi = 16°$ (which represents the orientation of the hexagon in the X–Y plane). Note that the polarization responses obtained in Figure 3 are the specific signature of threefold planar symmetry, and would be unattainable with a different multipolar symmetry.

The slight discrepancy between the model and the experiment regarding the shape and orientation of the four-lobed structure can be due either to the integration of the signals over the Rayleigh length of the objective focus (about 2 μm), or to interface effects between the crystal surface and the microscope slide. Deviations from Kleinman symmetry relations, due to the resonant conditions of the experiment, only slightly affected the four-lobed shapes and have thus been omitted from the model. In addition to confirming the molecular-order symmetry, the nonlinear optical responses of the crystal were also found to be perfectly uniform on scanning over the whole crystal surface area of the sample. The results of Figures 2,3 show, furthermore, that the oriented gas model, although not accounting for the strong π–π interactions between adjacent molecules, applies to the nonlinear response of the structure studied. This is mostly due to the nature of such interactions, which are locally centrosymmetric (although they contribute to the overall non-centrosymmetry) and provide a negligible contribution to the induced polarizations at the incident wavelength, 1028 nm.

In order to evaluate the SHG efficiency, $\|d\|$, of the octupolar crystal, we compared the SHG signal intensity of TTB to that of a reference 4-dimethylamino-*N*-methyl-4-stilbazolium tosylate (DAST)[19,20] crystal, which has very similar absorption characteristics (both crystals exhibit a cut-off wavelength at about 600 nm, with a large absorption centered at about 500 nm). The experimental data, corrected for the incident power, resulted in $\|d\|_{TTB} \approx 2 \times \|d\|_{DAST}$ at the 1028 nm incident wavelength. The DAST crystal is well-known for its very large efficiency ($\|d\|_{DAST} = 790 \times 10^{-9}$ esu at 1.55 μm from published data[21]); the TTB crystal is therefore among the most efficient organic crystals with $\|d\|_{TTB} \approx 1580 \times 10^{-9}$ esu under non-resonant conditions. The precision of this measurement was between 20 % and 30 % because of the sensitivity of the SHG signal to focalization and crystal positioning on the microscope slide. Note that the $\|d\|$ coefficients contain the molecular densities ($N_{TTB} = 9.92 \times 10^{20}$ molecules cm^{-3} and $N_{DAST} = 1.91 \times 10^{21}$ molecules cm^{-3} from the X-ray structure of the crystals), the local field factors, and the molecular β-efficiencies.

The molecular efficiency of the TTB molecule has been measured using the hyper-Rayleigh scattering (HRS) technique[22] in tetrahydrofuran (THF) (which is well adapted to octupolar molecules[11,12,23,24]) and led to $\beta_{111,TTB} = 407 \times 10^{-30}$ esu at zero frequency.[24] Assuming that the crystal refractive indices at wavelength, ω, are $n_1^\omega = n_2^\omega = 1.5$, and accounting for the crystal molecular density in the oriented gas model, we obtain $\|d\|_{TTB} = 2297 \times 10^{-9}$ esu at zero frequency, which is approximately three times larger than that of the DAST crystal. Such a factor is of the same order of magnitude as the one measured using nonlinear microscopy, with a discrepancy due to the error bars in the previous estimation and to the fact that the hyper-Rayleigh measurements were performed in solution where local field factors may have been different. The efficiency difference between DAST and TTB is mainly due to both the lower molecular efficiency of the dipolar DAST molecule (the highest published value is $\beta_{111,DAST} = 110 \times 10^{-30}$ esu at zero frequency[25]) and the less-favorable projection factors induced by the DAST unit-cell symmetry (which belongs to polar space group C_c[20]).

In conclusion, a rational design strategy, which takes advantage of favorable interlayer π–π interactions in stacked molecules, is proposed for the synthesis of an octupolar crystal with a large SHG efficiency. Optical polarization measurements of both SHG and TPF confirmed the non-centrosymmetric threefold symmetry of the TTB crystal, which allowed optimum use of the molecular hyperpolarizability components, resulting in a very large bulk nonlinearity.

Experimental

Optical Calibration Procedure: Previous studies [16] have shown that in the (X,Y,Z) framework, the exciting beam at the point of focus can be written as

$$\boldsymbol{E}(\Phi, \varepsilon, \delta, \omega t) = E \Big/ \sqrt{1 + \left(1 - \delta^2\right)} \times [\cos\Phi \cos\omega t, (1 - \delta) \sin\Phi \cos(\omega t + \varepsilon), 0] \quad (3)$$

where $\boldsymbol{E}$ is the field amplitude. The parameters δ and ε account respectively for the dichroism and ellipticity of the field polarization upon reflection by the dichroic mirror. They are measured separately by standard ellipsometry ($\varepsilon = 1.57$ rad and $\delta = -0.02$ at 1028 nm). The polarization direction, Φ, was varied from 0° to 360° by using a rotating half-wave plate inserted in the linear-excitation polarization control set-up. The DAST crystal, used as a reference, exhibited a quasi-identical absorption spectrum. The calibration of the nonlinear microscope efficiency was carried out using polarization measurements on a DAST crystal lying on its [001] face, which gave very specific polar patterns, for which the fits were in good agreement with the expected symmetry. This crystal could therefore have been considered for use as a reference in measurements of unknown $\|d\|$ values. The proportionality coefficient introduced to fit the SHG signals was indeed proportional to $\|d\|^2 P_{inc}^2$, where P_{inc} represents the peak power of the IR radiation incident on the crystal.

Received: March 25, 2004
Final version: July 23, 2004

[1] J. Zyss, *Nonlinear Opt.* **1991**, *1*, 3.
[2] J. Zyss, *J. Chem. Phys.* **1993**, *98*, 6583.
[3] J.-L. Oudar, D. S. Chemla, *J. Chem. Phys.* **1977**, *66*, 2664.

ADVANCED MATERIALS

[4] V. R. Thalladi, S. Brasselet, D. Bläser, R. Boese, J. Zyss, A. Nangia, G. R. Desiraju, *Chem. Commun.* **1997**, *19*, 1841.
[5] C. Andraud, T. Zabulon, A. Collet, J. Zyss, *Chem. Phys.* **1999**, *245*, 243.
[6] Y.-K. Lee, S.-J. Jeon, M. Cho, *J. Am. Chem. Soc.* **1998**, *120*, 10 921.
[7] J. Brunel, I. Ledoux, J. Zyss, M. Blanchard-Desce, *Chem. Commun.* **2001**, *10*, 923.
[8] C. Fiorini, F. Charra, J.-M. Nunzi, I. D. W. Samuel, J. Zyss, *Opt. Lett.* **1995**, *20*, 2469.
[9] S.-H. Kang, Y. S. Kang, W.-C. Zin, G. Olbrechts, K. Wostyn, K. Calys, A. Persoons, K. Kim, *Chem. Commun.* **1999**, *17*, 1661.
[10] S. Yokoyama, T. Nakahama, A. Otomo, S. Mashiko, *J. Am. Chem. Soc.* **2000**, *122*, 3174.
[11] H. Le Bozec, T. Le Bouder, O. Maury, A. Bondon, I. Ledoux, S. Deveau, J. Zyss, *Adv. Mater.* **2001**, *13*, 1677.
[12] V. R. Thalladi, S. Brasselet, H.-C. Weiss, D. Bläser, A. K. Katz, H. L. Carell, R. Boese, J. Zyss, A. Nangia, G. R. Desiraju, *J. Am. Chem. Soc.* **1998**, *120*, 2563.
[13] B. R. Cho, S. B. Park, S. J. Lee, K. H. Son, S. H. Lee, M.-J. Lee, J. Yoo, Y. K. Lee, G. J. Lee, T. I. Kang, M. Cho, S.-J. Jeon, *J. Am. Chem. Soc.* **2001**, *123*, 6421.
[14] Intermolecular distances relative to π–π interactions. Offset face to face π–π interactions: 1) For the benzene ring composed of carbon atoms C1 to C6 (bz(C1–C6)) and bz(C12–C17($-y+1$, $x-y$, $z+1/3$)): centroid separation = 4.832 Å; dihedral angle = 25.7°. 2) For bz(C1–C6) and bz(C1–C6($-y+1$, $x-y$, $z+1/3$, or $-x+y+1$, $-x+1$, $z-1/3$)): centroid separation = 5.115 Å; dihedral angle = 7.97°. 3) For bz(C12–C17) and bz(C36–C41($-x+y+1$, $-x+1$, $z-1/3$)): centroid separation = 5.464 Å; dihedral angle = 4.96°. Edge-to-face π–π interactions: 1) For bz (C12–C17) and bz(C24–C29($-y+1$, $x-y$, $z+1/3$)): centroid separation = 5.483 Å; dihedral angle = 63.1°. 2) For bz(C24–C29) and bz(C36–C41($-y+1$, $x-y$, $z+1/3$)): centroid separation = 5.303 Å; dihedral angle = 68.0°.
[15] A. I. Kitaigorodskii, *Molecular Crystals and Molecules*, Academic Press, New York **1973**.
[16] V. Le Floc'h, S. Brasselet, J.-F. Roch, J. Zyss, *J. Phys. Chem. B* **2003**, *107*, 12 403.
[17] J. Zyss, J.-L. Oudar, *Phys. Rev. A* **1982**, *26*, 2028.
[18] J. Zyss, S. Brasselet, V. R. Thalladi, G. R. Desiraju, *J. Chem. Phys.* **1998**, *109*, 658.
[19] H. Nakanishi, H. Matsuda, S. Okada, M. Kato, in *Proc. MRS Int. Meeting Adv. Mater.* Vol. 1 (Eds: R. F. C. Farrow, R. W. Siegel, A. M. Stacy), Materials Research Society, Warrendale, PA **1989**, p. 1.
[20] H. Oikawa, S. Fujita, H. Kasai, S. Okada, S. K. Tripathy, H. Nakanishi, *Colloids Surf., A* **2000**, *169*, 251.
[21] G. Knöpfle, R. Schlesser, R. Ducret, P. Günter, *Nonlinear Opt.* **1995**, *9*, 143.
[22] R. W. Terhune, P. D. Maker, C. M. Savage, *Phys. Rev. Lett.* **1965**, *14*, 681.
[23] T. Verbiest, K. Clays, A. Persoons, F. Meyers, J. L. Bredas, *Opt. Lett.* **1993**, *18*, 525.
[24] M. J. Lee, M. Piao, M.-Y. Jeong, S. H. Lee, , K. M. Kang, S.-J. Jeon, G. L. B. Tong, B. R. Cho, *J. Mater. Chem.* **2003**, *13*, 1030.
[25] K. Clays, B. J. Coe, *Chem. Mater.* **2003**, *15*, 642.

Tubular and Twisted Ni–P Fibers Molded from Morphology-Tunable and Recyclable Organic Templates of Hydrogen-Bonded Supramolecular Assemblages**

By *Masaru Nakagawa*,* *Daisuke Ishii*, *Ken'ichi Aoki*, *Takahiro Seki*, and *Tomokazu Iyoda*

Since the discovery of sheet-curled chrysotile,[1] polypyrrole,[2] and carbon nanotubes,[3] organic and inorganic tubular materials have attracted much attention due to their unique physical and chemical properties.[4] Template-directed synthesis is widely accepted as a simple, high-throughput, and cost-effective method for the fabrication of tubular fibers composed of metal sulfides and oxides,[5] metals,[6] or conducting polymers[7] through sol–gel polymerization,[8] electroless[9] or electrochemical[10] plating, or vapor deposition.[11] The inner surfaces of porous anodic alumina[12] and the outer surfaces of lipid-based cylindrical tubules,[13] organic gelator fibrils,[14] single- and double-headed amphiphile molecular assemblages,[15] carbon nanotubes,[16] and electrospun degradable polymer fibers[17] have been utilized as reliable templates for the fabrication of tubular fibers. Many efforts are currently being made to control the inner diameter and even the entire morphology of these tiny tubular materials.

We have reported previously that the amphoteric compound 6-[2-propyl-4-(4-pyridylazo)phenoxy]hexanoic acid (**1**, Fig. 1) self-organizes upon neutralization of its alkaline aqueous solution to give fibrous molecular assemblages.[18a] Atomic force microscopy (AFM) revealed that the dried fibrous molecular assemblages have an almost uniform submicrometer diameter of around 400 nm. During the neutralization, a

[*] Prof. M. Nakagawa, D. Ishii, Prof. T. Iyoda
Chemical Resources Laboratory
Tokyo Institute of Technology
4259 Nagatsuta, Midori-ku, Yokohama 226-8503 (Japan)
E-mail: mnakagaw@res.titech.ac.jp
Dr. K. Aoki
Faculty of Science
Toho University
Funabashi, Chiba 274-8510 (Japan)
Prof. T. Seki
Department of Applied Chemistry
Graduate School of Engineering
Nagoya University
Chikusa, Nagoya 464-8603 (Japan)
Prof. T. Iyoda
CREST-JST
JST, 4-1-8 Honmachi, Kawaguchi, Saitama 332-0012 (Japan)

[**] This study was carried out at the Chemical Resources Laboratory of the Tokyo Institute of Technology. We thank Yukari Dan of Hitachi Science System, Ltd. and Hidehiro Yamada of Hitachi High-Technologies Corporation for their assistance with the SEM observations. We also thank Taichi Nagashima and Mitsuhide Yamada of Osaka Gas Ltd. for their help with the XPS measurements.

  DOI: 10.1002/adma.200400520